p53 regulates cell survival by inhibiting PIK3CA in squamous cell carcinomas

Bhuvanesh Singh,[1,5] Pabbathi G. Reddy,[1] Andy Goberdhan,[1] Christine Walsh,[3] Su Dao,[1] Ivan Ngai,[1] Ting Chao Chou,[2] Pornchai O-charoenrat,[1] Arnold J. Levine,[3] Pulivarthi H. Rao,[4] and Archontoula Stoffel[3,5]

[1]Laboratory of Epithelial Cancer Biology and [2]Preclinical Pharmacology Core Facility, Memorial Sloan-Kettering Cancer Center, New York, New York 10021, USA; [3]Laboratory of Cancer Biology, Rockefeller University, New York, New York 10021, USA; [4]Children's Cancer Center, Baylor College of Medicine, Houston, Texas 77030, USA.

Interactions between the *p53* and *PI3K/AKT* pathways play a significant role in the determination of cell death/survival. In benign cells these pathways are interrelated through the transcriptional regulation of *PTEN* by *p53*, which is required for *p53*-mediated apoptosis. *PTEN* exerts its effects by decreasing the phosphorylated *AKT* fraction, thereby diminishing prosurvival activities. However, the link between these pathways in cancer is not known. In this study, *PIK3CA*, encoding the p110α catalytic subunit of *PI3K*, is identified as an oncogene involved in upper aerodigestive tract (UADT) carcinomas. Simultaneous abnormalities in both pathways are rare in primary tumors, suggesting that amplification of *PIK3CA* and mutation of *p53* are mutually exclusive events and either event is able to promote a malignant phenotype. Moreover, the negative effect of *p53* induction on cell survival involves the transcriptional inhibition of *PIK3CA* that is independent of *PTEN* activity, as *PTEN* is not expressed in the primary tumors. Conversely, constitutive activation of *PIK3CA* results in resistance to p53-related apoptosis in *PTEN* deficient cells. Thus, *p53* regulates cell survival by inhibiting the *PI3K*/*AKT* prosurvival signal independent of *PTEN* in epithelial tumors. This inhibition is required for p53-mediated apoptosis in malignant cells.

[*Key Words*: P53; PI3K; cell survival; squamous cell carcinomas; head and neck neoplasms; lung neoplasms]

Received December 31, 2001; revised version accepted February 22, 2002.

Upper aerodigestive tract malignancies (UADT), including tumors arising from the head and neck, lung, and cervical esophagus, account for 18% of all cancers and 33% of all cancer deaths annually in the United States (Greenlee et al. 2000). These malignancies share a complement of genetic aberrations, hallmarked by a high prevalence of mutations in *p53* (Hollstein et al. 1997). The p53 protein provides critical antagonism to tumor development by inhibiting damaged cells from progressing through the cell cycle or promoting apoptosis (Levine et al. 1994). These features explain why it is often mutated and thereby inactivated in human malignancies.

Whole genome characterization of UADT tumors by comparative genomic hybridization (CGH) identified gain and amplification at 3q with a high prevalence at chromosomal bands 3q26–q27 (Bjorkqvist et al. 1998; Knuutila et al. 1998; Shinomiya et al. 1999; Singh et al. 2001). This locus is of particular interest, as it has a high prevalence in multiple cancer types, displays a predilection for UADT cancers, and its presence is associated with detrimental biological and clinical consequences. Although prior studies have identified candidate genes at the 3q locus, controversy still exists regarding the gene(s) that are the target of this amplification. The *PIK3CA* gene, located at 3q26, encodes the catalytic subunit (p110α) of a class I_A *PI3K*, one component of a lipid-signaling pathway involved in multiple cancer-associated functions including cell survival, proliferation, cell migration, vesicle trafficking, and vesicle budding. *PIK3CA* was proposed as an oncogene in cervical and ovarian cancer, but its involvement in UADT remains unclear (Shayesteh et al. 1999; Ma et al. 2000).

In this study the presence of two independent peaks of high-level amplification at 3q26.3, contained within two BAC clones is demonstrated. The alpha catalytic subunit of phosphoinositide-3-kinase (*PIK3CA*) is identified as a candidate oncogene involved in one of the amplified peaks in UADT carcinomas. The presence of the *PIK3CA* gene in a peak of amplification at 3q26.3, with corresponding RNA and protein expression, increased phosphorylated AKT protein in both cell lines and primary tumors, as well as the effects of *PI3K* inhibition, strongly implicate *PIK3CA* as one of the genes responsible for the biological consequences associated with the 3q amplification.

[5]Corresponding authors.
E-MAIL singhb@mskcc.org; FAX (212) 717-3302.
E-MAIL stoffea@rockvax.rockefeller.edu; FAX (212) 327-7058.
Article and publication are at http://www.genesdev.org/cgi/doi/10.1101/gad.973602.

Simultaneous mutations in *p53* and amplification of *PIK3CA* are not found in the same tumors, strongly indicating that mutations in either pathway can render the cell refractive to programmed cell death and prone to transformation.

In normal mouse fibroblasts, several studies suggest a negative regulation of the *PI3K/AKT* pathway by *p53* through the transcriptional activation of *PTEN* (Franke et al. 1997; Sabbatini and McCormick 1999; Stambolic et al. 2001). *PTEN* antagonizes *PI3K* function by dephosphorylating phosphoinositol triphosphate (PIP3), resulting in the reduction in the phosphorylated AKT fraction and G_1 arrest (Wymann and Pirola 1998).

Systematic analysis of the effects of *p53* on *PIK3CA* in EB1 colon cancer cells after UV induction shows its ability to regulate cell survival by inhibiting *PIK3CA* in a *PTEN*-dependent manner. Conversely, in UADT tumors, an alternative pathway for the inhibition of the *PI3K/AKT* survival pathway through *p53* results from the transcriptional down-regulation of *PIK3CA* by *p53* in a *PTEN*-independent manner. Moreover, it appears that the coordinated inhibition of *PI3K/AKT* is essential for the progression of *p53*-related apoptosis in *PTEN* deficient systems.

Results

PIK3CA *as an oncogene in UADT carcinomas*

Amplification of the 3q26–27 region is a common and crucial event in UADT carcinomas. To refine this region and identify the oncogene(s) within the 3q26–27 amplicon, 73 YAC clones were isolated spanning ~38 cM within chromosomal bands 3q26–27. Sequential dual-color FISH with 43 of the identified YAC clones was performed on cell line MDA886, which contains the minimal amplified region identified by CGH. Based on this analysis, the apex of amplification was restricted within three highly amplified, overlapping YAC clones (803E3, 940H11, 923E6) at 3q26.3 with copy numbers ranging from 8–10. The size of the genomic segment was determined by pulse field gel electrophoresis (PFGE) analysis of these clones and spans ~1.5–2.0 Mb. To further characterize the amplification region, 39 BACs were isolated spanning the region between D3S3511 and WI-6165. Sequential dual-color FISH was performed on cell line MDA886 using all 39 BAC clones. Ten BAC clones associated with high-level amplification in MDA886 were subsequently used to screen four additional head and neck carcinoma cell lines known to harbor 3q amplification based on CGH analysis. Two independent amplification peaks were identified within BAC clones 202B22 and 386M7, with mean copy numbers of 10.6 and 10.3, respectively (Fig. 1). Analysis of BAC 386M7 showed the presence of a single gene, *PIK3CA*, which encodes the p110α catalytic subunit of *PI3K*. To identify the prevalence of *PI3KCA* amplification, FISH analysis was performed on 20 primary tumors and 21 cell lines derived either from head and neck or lung carcinomas, using BAC 386M7 as a probe. The presence of amplification was confirmed in 13 out of 21 cell lines (62%) with copy numbers ranging from 5–13. In addition, high-level amplification of *PIK3CA* was identified in six out of the 20 primary tumors (30%) analyzed by FISH (Table 1).

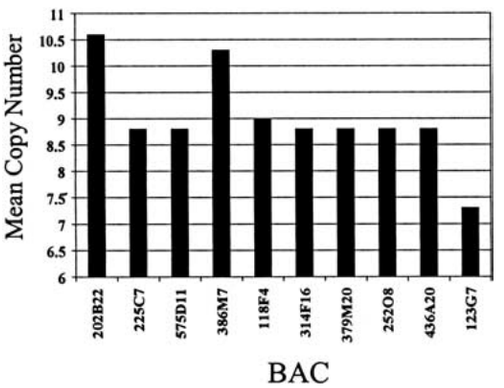

Figure 1. Identification of two amplification peaks at 3q26.3. FISH analysis with BAC genomic clones, of five head and neck squamous-cell carcinoma cell lines containing 3q26–27 amplification, identified two independent amplification peaks within BAC clones 202B22 and 386M7.

To demonstrate the role of *PIK3CA* as an oncogene in UADT malignancies, semiquantitative PCR and Western blot analyses were performed on 13 head and neck and lung cancer cell lines and six primary tumors with *PIK3CA* amplification. Increased RNA and protein expression levels of p110α were observed in 11 out of 13 cell lines and in all primary tumors examined (Fig. 2). Phosphorylated *AKT* expression, the downstream target of *PIK3CA*, was present in all cases that exhibited high p110α protein levels, as expected. In addition, using RT–PCR, we detected 4× or greater increase in p110α mRNA expression in 10 of 32 (31%) squamous cell carcinomas and two of 12 (17%) adenocarcinomas of the lung relative to normal lung controls. The predilection of PIK3CA expression for squamous cell histology is congruent with the reported pattern of 3q amplification in lung cancers (Bjorkqvist et al. 1998).

To investigate the biological effects of increased *PIK3CA* activity in aerodigestive tract carcinomas, six cell lines derived from head and neck or lung carcinomas with differential degrees of *PIK3CA* expression were treated with the *PI3K* specific inhibitor LY294002. Treatment with LY294002 produced a dose-dependent decrease in cell viability in all of the cell lines. The degree of response correlated with the basal level of *PIK3CA* expression (Fig. 2). A dose-dependent decrease in phosphorylated fraction of AKT also resulted from *PI3K* inhibition (Fig. 2).

The oncogenic potential of *PIK3CA* was also demonstrated by transfection of a constituently active *PIK3CA* (myrPIK3CA) in 3T3 cells. Transfection resulted in changes characteristic of malignant transformation, including increased growth rate, morphological changes, and growth in serum deficient media (Fig. 3). Anti-sense

Table 1. *Status of PIK3CA and pathway components in primary head and neck squamous cell carcinomas*

Sample	Tobacco use	PIK3CA amplification by FISH[a]	PIK3CA RT–PCR[b]	PI3K–p110α Western blot	Phospho-AKT	Mutation p53	Mutation PTEN	Methylation PTEN	PTEN Western blot[b]
4TU	+	–	–	–	–	+	–	–	↓
29TU	+	–	–	–	–	–	–	–	↓
34TU	+	–	–	–	–	+	–	–	↓
39TU	+	+	+	+	+	–	–	–	↓
40TU	+	–	–	–	–	+	–	–	↓
47TU	+	+	+	+	–	–	–	–	↓
63TU	+	–	–	–	–	–	–	–	↓
86TU	–	–	–	–	–	+	–	–	↓
97TU	+	+	+	+	+	–	–	–	↓
117TU	+	–	–	+	–	–	–	–	↓
121TU	–	–	+	+	–	+	–	–	↓
140TU	–	–	–	–	–	–	–	–	↓
141TU	+	–	–	–	–	–	–	–	↓
150TU	–	–	–	–	+	–	–	–	↓
153TU	–	–	–	–	–	+	–	–	↓
158TU	+	–	–	–	+	–	–	–	↓
163TU	+	+	+	+	+	–	–	–	↓
166TU	+	+	+	+	+	–	–	–	↓
171TU	–	–	–	–	–	–	–	–	↓
183TU	+	+	+	+	+	–	–	–	↓

[a]FISH performed using 386M7 BAC containing PIK3CA as the probe.
[b]Expression reported relative to matched normal control.

PIK3CA transfection into UADT cell lines was highly toxic, resulting in cell death in all but one of the four cell lines where stable transfections were performed. The transfection of antisense to *PIK3CA* (asPIK3CA) into MDA886 cells resulted in morphological changes, decreased growth rate (6.6-fold reduction in growth rate at 72 h), increased cell death (see Fig. 5, below), sensitivity to serum deficient conditions (7.1-fold increase in cell death at 72 h), and loss of ability to form colonies in soft agar (62% vs. 2% colony formation) when compared with control cells. The asPIK3CA-transfected MDA886 cells were highly sensitive to p53, with even low-level induction of UV exposure resulting in complete cell death (see Fig. 5, below).

PIK3CA *and* PTEN *are regulated by* p53 *in EB1 cells*

PTEN is a tumor suppressor gene and a negative regulator of *AKT*, which is required for p53-mediated apoptosis in immortalized mouse embryonic fibroblasts. As in many other types of cancer, the most common genetic aberration in UADT carcinoma is mutations in the *p53* gene. To delineate the mechanisms of *PIK3CA* regulation in cancer cells, we investigated its functional interactions with *p53* and *PTEN* utilizing a colon cancer derived *p53*-inducible cell system. *p53* was induced in EB1 cells by the introduction of 100 μM zinc, resulting in transcriptional activation of *p21* and *MDM2*, as well as apoptosis (Fig. 4). A fourfold induction in *PTEN* expression was observed, with the highest levels occurring at 20–24 h post-*p53* induction. Conversely, a sixfold downregulation of *PI3K p110*α expression was detected by both Northern and Western blot analyses with minimal levels at 12–16 h post-*p53* induction. A progressive decrease in phosphorylated *AKT* levels resulted from the *p53*-related *PTEN* induction and *PIK3CA* inhibition. The cotreatment of EB1 with LY294002, a specific *PI3K* inhibitor, and induction of *p53* by zinc at levels associated with apoptosis resulted in strong synergism. A reduction in the level of *p53* induction by 6.2-fold (dose reduction index) was sufficient to induce an equivalent degree of cell death when cotreated with *PIK3CA* inhibitor compared with *p53* induction alone (Fig. 4). Taken together, these results indicate an association of the *PI3K* and *p53* pathways in cell death induction in a *PTEN*-dependent manner.

PIK3CA *regulation by* p53 *in* PTEN *intact and deficient cells*

To investigate whether the interaction of the *PI3K* and *p53* pathways is *PTEN*-dependent in UADT carcinomas, 16 cell lines and 20 primary tumors were subjected to PTEN gene sequencing, promoter methylation analysis, and protein expression assessment (Tables 1, 2). Mutation or promoter methylation of *PTEN* was seen in only one cell line each, both derived from lung cancers. However, PTEN protein was not detected in any of the head and neck cancer cell lines analyzed and was diminished at least threefold in all primary tumors relative to the matched mucosal control. In the same tumors, *p53* mutations were sought by sequencing the exons containing the DNA binding domain, which is most frequently mutated in cancers. Mutations of *p53* were found in 30% of

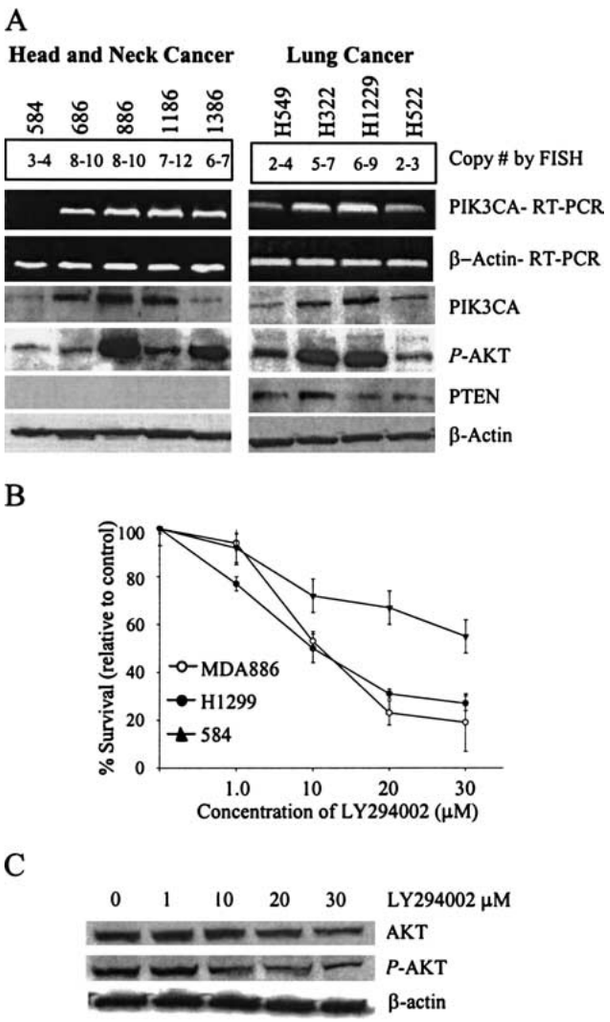

Figure 2. (*A*) Correlation between PIK3CA amplification, expression, and function. A high degree of correlation was detected between PIK3CA copy number by FISH, RNA expression (semiquantitative RT–PCR), and protein expression (Western blot analysis) in head and neck (*left*) and lung (*right*) carcinoma cell lines. Elevated PI3K 110α expression corresponded with phosphorylated AKT levels. PTEN protein was not detected in head and neck carcinoma derived cell lines. (*B*) Impact of PI3K inhibition. The impact of PI3K inhibition by LY294002 on cell viability was measured by the MTT assay. A dose-dependent sensitivity was detected in all cell lines, but was highest in cell lines containing high-level PIK3CA amplification. (*C*) Reduction of phosphorylated AKT protein levels in MDA886 resulted from PI3K inhibition by LY294002.

the primary tumors and 69% of cell lines analyzed. None of the tumors containing mutations in *p53* were found to have amplified *PIK3CA*, indicating a mutually exclusive selection of mutations in either pathway ($P = 0.077$; 95% confidence interval = 0.00–0.20; SURGISTAT software). However, there was significant heterogeneity in the p53 and PIK3CA status in the examined cell lines, reflecting their advance genomic composition.

The effects of *p53* induction by UVB on *PTEN* and *PIK3CA* transcription were assessed in cell lines derived from UADT carcinomas with intact or absent PTEN protein expression (Fig. 5). In cell line A549, induction of wild-type p53 resulted in the expected decrease in *PIK3CA* and increase in PTEN protein levels. The effects on phosphorylated *AKT* levels were similar to that seen in EB1 cells. This resulted in synergism in the induction of cell death. Synergism between *PIK3CA* and *p53* was present at all dose levels.

In cell line 886, which has no detectable *PTEN* protein levels, the induction of *p53* still resulted in a decrease in *PIK3CA* expression and reduction in the phosphorylated AKT levels. The synergistic activity between *p53* induction and *PI3K* inhibition remained, but was more dose-dependent and was seen at higher levels of *p53* induction.

To determine the effect of *PIK3CA* inhibition on the *p53* proapoptotic activity, we transfected a constituently active *PIK3CA* mutant into MDA886. This resulted in resistance to cellular death as a consequence of *p53* induction by UVB and had no effects on the phosphorylated *AKT* levels. These results strongly indicate that the *p53* role in regulation of cellular survival (*PI3K*) in epithelial tumors is independent of *PTEN*, which is largely not expressed in these cells or tumors.

Discussion

The *PI3K/AKT* cascade has been implicated in promoting cell survival downstream of extracellular stimuli (Franke et al. 1997; Wymann and Pirola 1998; Datta et al. 1999). These stimuli mediate intracellular signaling through ligation of transmembrane receptors. Activation of these receptors results in the recruitment of *PI3K* isoforms to the plasma membrane that subsequently generate 3′-phosphorylated phosphoinositides (PI3,4P, PI3,4,5). Phosphoinositol triphosphate subsequently activates *PDK1*, resulting in phosphorylation of AKT. Phosphorylated AKT is the active component of the pathway and has multifactorial effects resulting in the promotion of cellular survival through the inactivation of proapoptotic genes by phosphorylation.

In this study the minimal amplified region at 3q26.3 in head and neck tumors was identified in a positional cloning approach utilizing YAC and BAC clones spanning the 3q amplicon. Sequence analysis of the BAC clone with the highest amplification detected by FISH, identified *PIK3CA* as the candidate oncogene within the minimal amplified region. *PIK3CA* encodes for the p110α catalytic subunit of *PI3K*, which forms a heterodimer with the p85-regulatory subunit and is sequestered to the cell membrane in response to multiple stimuli. Increased RNA and protein levels of PIK3CA and phosphorylated AKT, the downstream target of *PIK3CA* in primary tumors and cell lines, show that *PIK3CA* is not only amplified at the genomic level but also transcriptionally and translationally activated through the amplification. Inhibition of *PIK3CA* activity in six cell lines established from head and neck or lung carcinomas hav-

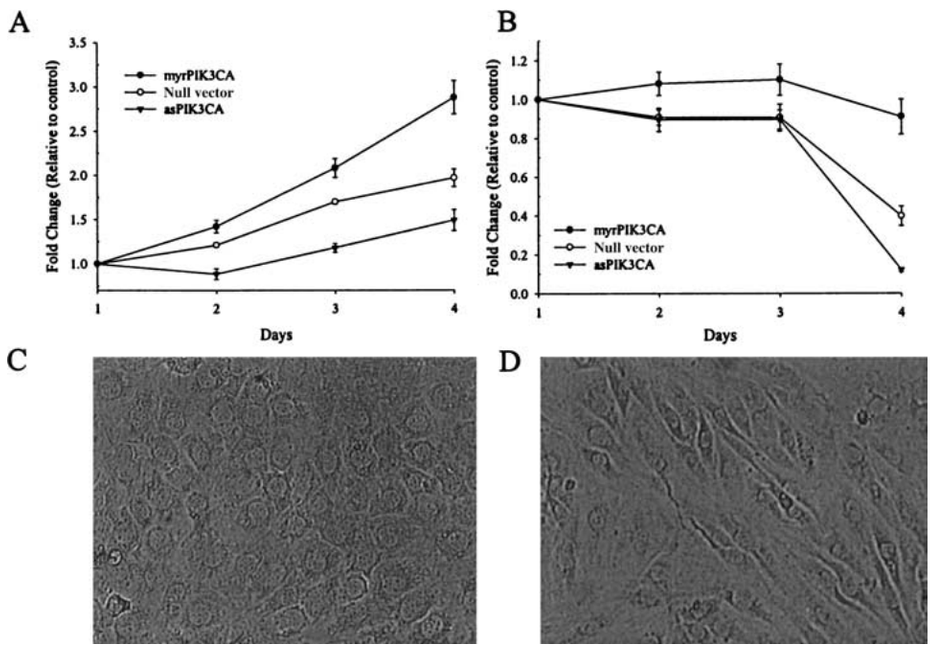

Figure 3. Transformation of 3T3 cells by PIK3CA. (*A*) myrPIK3CA- or asPIK3CA-transfected 3T3 cells were subjected to cell viability measurement with the MTT assay (±1 standard deviation) showing significantly enhanced growth in myrPIK3CA-transfected cells and a growth reduction in cells transfected with asPIK3CA. (*B*) Preservation of growth in serum deficient media was seen in myrPIK3CA-transfected cells. (*C*) Transfection of myrPIK3CA results in changes associated with dedifferentiation, including loss of spindle cell morphology and contact growth inhibition, compared with the null vector transfected (*D*) cells.

ing differential degrees of *PIK3CA* expression produced a dose-dependent decrease in cell viability. The degree of response correlated with the basal level of *PIK3CA* expression and a dose-dependent decrease in phosphorylated fraction of AKT protein followed *PI3K* inhibition, suggesting a functional pathway for the observed impact on cellular viability. In addition, *PIK3CA* transfection into 3T3 cells led to morphological changes, abnormal growth, and development of colonies on soft agar. Finally, the abrogation of the malignant phenotype in MDA886 cells by transfection of antisense to *PIK3CA* confirms its oncogenic potential.

In summary, several lines of evidence strongly suggest that *PIK3CA* is the target of the 3q amplification: (1) the identification of *PIK3CA* within the minimal amplified region at 3q, (2) the correlation between RNA and protein expression of *PIK3CA*, (3) the corresponding high-level expression of phosphorylated AKT with gene amplification in both cell lines and primary tumors, (4) the deleterious effects in *PI3K* inhibition in cases with high-level expression, and (5) transformation of 3T3 cells after *PIK3CA* transfection. Given the presence of two independent peaks of amplification in the minimal common region, it remains possible that another oncogene(s) may reside at the 3q26.3 locus.

p53 is disrupted by mutations in many tumors and is also commonly altered in UADT tumors. Sequencing of primary tumors and cell lines detected mutations of the *p53* DNA binding domain in 47% of all cases. Interestingly, none of the tumors that exhibited *p53* mutations showed simultaneous amplification of *PIK3CA* and vice versa (Table 1). This suggests that both pathways may be functionally redundant and complement each other in UADT carcinomas.

In benign cells several lines of evidence have suggested a role for *p53* in negative regulation of cellular survival via binding to the *PTEN* promoter (Sabbatini and McCormick 1999; Henry et al. 2001). *PTEN* suppresses the *PI3K/AKT* survival signaling by dephosphorylating phosphoinositol triphosphate with subsequent reduction of the phospho-AKT fraction and G_1 arrest (Cantley and Neel 1999; Ramaswamy et al. 1999). In EB1 colon cancer cells, *p53* induction resulted in a significant down-regulation of *PI3K/AKT*. Furthermore, simultaneous *PIK3CA* inhibition showed strong synergism in *p53*-mediated apoptosis, and *p53* induction levels were decreased by 6.2-fold (dose reduction index) with an equivalent degree of cell death. *PTEN* mRNA and protein levels correlated with the induced *p53* levels, strongly suggesting that the negative regulation of p53 on the *PI3K/AKT* survival signal is *PTEN*-dependent in these cancer cells. Conversely, there was no detectable *PTEN* protein in head and neck cancer cell lines and *PTEN* expression was diminished at least threefold relative to the matched mucosal control in all primary tumors. Induction of *p53* in this tumor resulted in a decrease in *PIK3CA* expression and reduction in the phosphorylated AKT levels. The synergistic activity between *p53* induction and *PI3K* inhibition remained, but was more dose-dependent and was seen at higher levels of

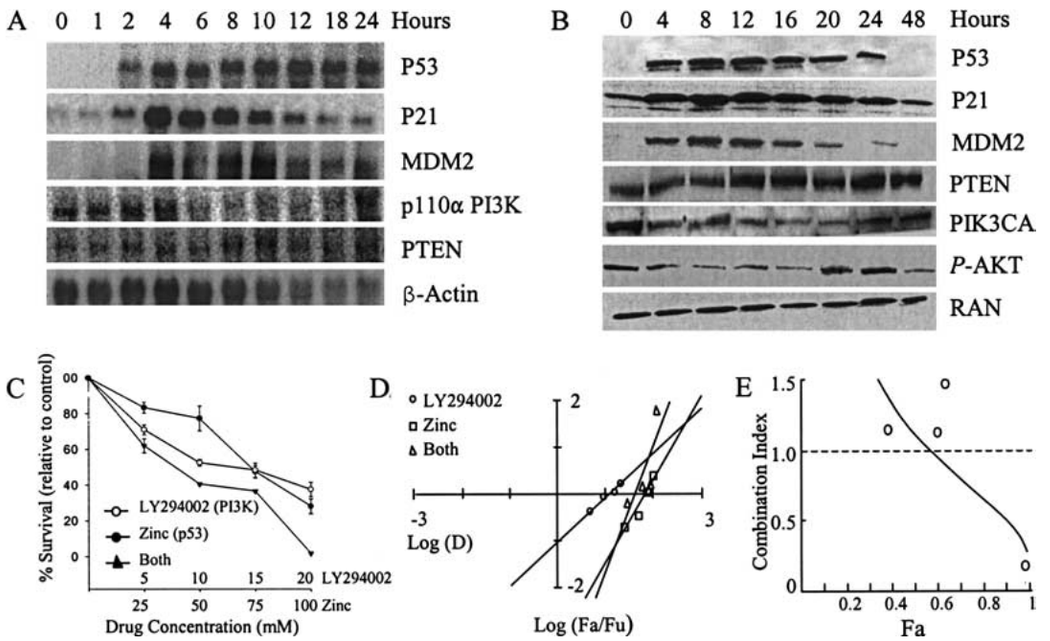

Figure 4. Effects of p53 induction on PI3K-p110α and PTEN expression. Northern (*A*) and Western (*B*) blot analyses of EB1 cells induction of p53 by 100μM zinc resulted in transcriptional activation of p21 and MDM2. A fourfold induction in PTEN expression and a sixfold down-regulation of *PIK3CA* expression was detected by both Northern and Western blot analyses. A decrease in phosphorylated AKT levels resulted from the p53-related PTEN induction and PIK3CA inhibition. (*C*,*D*,*E*) Results from analysis of synergism between p53 induction and PI3K inhibition. Significant synergism was demonstrated with p53 induction by zinc and PI3K inhibition with LY294002 in EB1 cells.

p53 induction. Finally, resistance to *p53*-related apoptosis by transfection of a constituently active *PIK3CA* in MDA886 suggests that the coordinated inhibition of *PI3K/AKT* is essential for *p53* related apoptosis in these cells and tumors.

These results strongly argue that the role of *p53* in the regulation of cellular survival pathway (*PI3K/AKT*) involves its effects on both PTEN and PIK3CA. In head and neck tumors, the effects of *p53* on *AKT* is largely independent of its effect on *PTEN*, as its ex-

Table 2. *Status of PIK3CA and pathway components in cell lines derived from lung and head and neck carcinomas*[a]

Cell line	PIK3CA amplification by FISH[b]	PIK3CA RT–PCR	PI3K–p110α Western blot	Phospho-AKT	Mutation p53	Mutation PTEN	Methylation PTEN	PTEN Western blot
584	2-3	–	–	+	–	–	–	–
MDA686	8-9	++	++	+	+	–	–	–
MDA886	9-12	+++	+++	+++	–	–	–	–
MDA1186	7-11	+++	++	++	+	–	–	–
MDA1386	5-9	++	+	+++	+	–	–	–
MDA1586	3-4	+	+	+	+	–	–	–
MDA1986	2-3	+	+	+	–	–	–	–
MSKQLL2	4-5	+	+	+	+	–	–	–
NIH H157	2-3	+	+	+	+	+	–	+
NIH H322	3-8	+++	++	+++	+	–	–	++
NIH H1299	4-7	+++	++	+++	+	–	–	+
NIH H522	2-3	+	+	+	+	–	–	+
NIH H520	5-10	++	++	++	+	–	+	–
NIH H2030	4-5	++	+	++	–	–	–	+
NIH H549	2-3	+	+	++	–	–	–	++
NIH H2170	2-3	++	+	+	+	–	–	+

[a]Note FISH was performed on 21 individual cell lines. Representative cell lines undergoing detailed characterization are shown in this Table.
[b]FISH performed using 386M7 BAC containing PIK3CA as the probe.

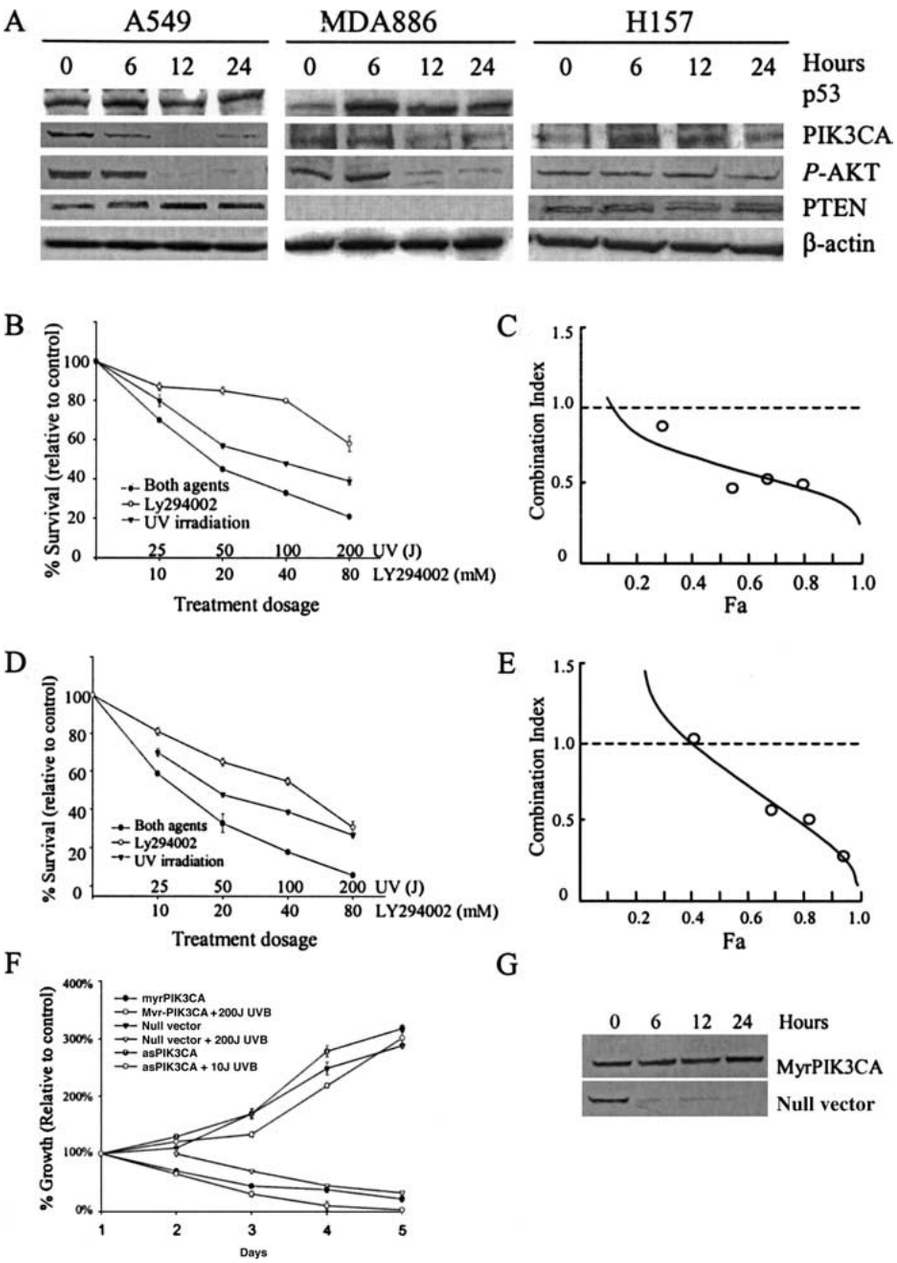

Figure 5. (*A*) Western blot analysis of cell lines exposed to 200J of ultraviolet irradiation (UV). In A549, with wild-type p53 and intact PTEN protein expression, UV exposure resulted in increased p53 protein expression and related increase in PTEN and decrease in PI3K p110α and phosphorylated AKT levels. In cell line MDA886, containing wild-type p53 and no PTEN protein expression, UV exposure resulted in a decrease in PI3K p110α and phosphorylated AKT protein levels. In cell line H157, containing mutated p53 and PTEN, UV irradiation had no effects on PI3K p110α, or AKT protein levels. (*B*,*C*) Synergism analysis between p53 induction and PI3K inhibition in cell line A549 showing cell viability (*B*) and isobologram (*C*). Synergism was identified at all dose levels. (*D*,*E*) Synergism analysis in cell line MDA 886. Synergism was detected in a dose dependent manner and to a greater extent than in cell line A549. (*F*,*G*) Transfection of myrPIK3CA into MDA886 results in resistance to p53-related apoptosis, as shown in growth curve F and abrogates p53-related decrease in phosphorylated AKT compared to null vector detected by Western blotting (*G*). Transfection of asPIK3CA into MDA886 cells resulted in rapid cell death and increased sensitivity to UV irradiation (*F*).

pression is absent or significantly reduced in these tumors. Further studies will determine if the interaction between p53 and *PIK3CA* is direct or if intermediate steps involving a signal mediator are required for the observed inhibitory role of p53 on *PIK3CA* transcription and cell survival. The relationship between *p53* and *PIK3CA* described in this work offers novel and valuable insights into the process of tumorigenesis and

could well aid in the design and development of cancer treatments.

Materials and methods

Cell lines and tissue resources

Cell lines derived from head and neck squamous cell carcinomas were kindly provided by Dr. P.G. Sacks (New York University School of Dentistry, New York, NY) and those derived from lung carcinomas were purchased from the American Type Tissue Collection. EB1 is a colon tumor-derived cell line carrying a wild-type *p53* gene under the control of an inducible metallothionein promoter (Shaw et al. 1992; Zhao et al. 2000). Induction with 100 μM zinc chloride results in sustained high levels of p53 expression and the induction of progressive apoptosis. Tumor specimens utilized in the study were obtained from sequential patients undergoing resection of carcinomas of the oral cavity or lung at Memorial Sloan-Kettering Cancer Center, following institutional guidelines. Normal mucosal tissue was also obtained from the margins of surgical resection. All tissue was snap frozen in liquid nitrogen immediately after resection and stored until use.

Analysis of amplification

YAC and BAC clones were identified by screening computerized resources at The Whitehead Institute for Biomedical Research/MIT Center for Genome Research (www.genome.wi.mit.edu) and the San Antonio Genome Center (http://apollo.utscsa.edu) as described previously (Zhao et al. 1997; Stoffel et al. 1999). Individual YAC and BAC clones were either purchased from a commercial source (Research Genetics) or kindly provided by Dr. Susan Naylor (The University of Texas Health Science Center at San Antonio). YAC and BAC clones were mapped to the 3q region and tested for chimerism by FISH on metaphase spreads from normal lymphocytes. The relative position of the YAC and BAC clones was accomplished by STS content PCR screening and sequential dual-color FISH analysis as described previously (Zhao et al. 1997; Stoffel et al. 1999). BAC sequences were obtained from The Human Genome Sequencing Center at the Baylor College of Medicine (www.hgsc.bcm.tmc.edu). PFGE was used to determine the size of the genomic insert according to manufacturer's protocol (Bio-Rad Laboratories).

FISH

FISH was performed and images analyzed as described previously (Singh et al. 2001).

Sequence generation

The following primers were generated using the Primer 3 program (http://www-genome.wi.mit.edu/cgi-bin/primer/primer3_www.cgi): human β-*actin* (accession no. XM-037239), 5′-TGGGACGACATGGAGAAAATC-3′, 3′-AGGGAGGAGCTGGAAGCAGC-5′; human *PIK3CA* (accession no. Z29090), 5′-TGTGGGACTTATTGAGG-3′, 3′-CACCATGATGTGCATCATTCA-5′. Sequencing of *p53* (exons 4–9) and *PTEN* (exons 1–9) was performed with exon-specific primers according to manufacturer's protocol or as described previously (BD Biosciences Clontech; Liaw et al. 1997).

Semiquantitative and RT–PCR

A single step RT–PCR kit was utilized for amplification following the manufacturer's protocols (GIBCO BRL Life Technologies). PCR products were gel purified and confirmed by direct sequencing. Semiquantitative PCR was performed as described previously (Bhuyan et al. 2000). RT–PCR was performed on the iCycler iQ Real-Time Detection System (Bio-Rad Laboratories) using SYBR green detection and beta-actin for control as per manufacturer's protocols (QIAGEN).

Northern blot analysis

Twenty micrograms of total cellular RNA was extracted, size fractionated on a 1.2% agarose/formaldehyde gel, and transferred to a nylon membrane (Oncor). Hybridization was performed using standard procedures. Probes were generated for cDNA clones for *PTEN* (IMAGE: 322160), *PI3K* (IMAGE: 345430), *p53* (1.6-kb insert from human *p53* complete cDNA), *p21* (0.5-kb *Not*I insert of human *p21* complete cDNA), and *MDM2* (2.1-kb insert from human *MDM2* complete cDNA). For quantitation of the amount of mRNA, the Northern blots were hybridized with a human β-*actin* probe (Clontech).

SDS-PAGE and Western blot analysis

Proteins were resolved on SDS–polyacrylamide gels under reducing conditions and blotted onto nylon membranes (Bio-Rad Laboratories) for Western analysis according to standard procedures. Rabbit polyclonal antibodies against p110α subunit of *PI3K*, *PTEN*, *AKT*, and phospho–*AKT* (Cell Signaling Technology), goat polyclonal antibodies against β-*actin* and *PIK3CA*, and monoclonal antibodies against *p53* (Pab1801 [1:2]), *MDM2* (4B11 [1:2]), and *p21* (C19) were generated in the laboratory or obtained from a commercial source and utilized according to the manufacturer's protocols (Santa Cruz Biotechnology).

PTEN promoter methylation analysis

Promoter methylation studies were performed as described previously (Salvesen et al. 2001).

Cell viability assays

Cells were plated in 96-well plates at a density of 1×10^5 and treated with ultraviolet radiation, zinc, and/or LY294002 in parallel with appropriate controls. UVB irradiation was delivered using a Spectroline Shortwave UV source (Spectronics Corporation) and dose estimated using a Traceable Ultra Violet light meter (Fisher Scientific). After treatment, the cells were incubated in solution containing 3-(4,5-dimethylthiazol-2yl)-2,5-diphenyl-2H tetrazolium bromide at a concentration of 0.4 mg/mL for 4 h. MTT values were measured on a MicroELISA reader (Dynatech Laboratories) at OD_{570}. Cellular viability was calculated relative to the control group.

Transfection

Constituently active PIK3CA (myrPIK3CA) was generated using a murine *PI3K* p110α under the control of the CMV promoter in pUSEamp, activated by the addition of the avian src myristoylation sequence (MGSSKSKPK) at the N terminus (Upstate Biotechnology). Antisense to the full-length *PI3K* p110α cDNA (asPIK3CA) was generated as described previously (Alper et al. 2000). Cells were transfected with pUSEamp vector without an insert to serve as a control (nvPIK3VA). Transfections

were performed using the Lipofectamine Plus Reagent Kit according to the manufacturer's protocols (GIBCO BRL), under neomycin selection for stable transfection.

Analysis of synergism

To determine whether synergistic, additive, or antagonistic effects were achieved in vitro, cell lines were treated both singly and with two modes of treatment in combination. The combination ratio was selected near the IC_{50} ratio for each agent. Each drug and their combinations at five serial twofold dilution concentrations were used for cell growth inhibition assays to generate dose-effect relationships. The median-effect plot and the combination index (CI)-isobologram method of Chou-Talalay (Chou and Talalay 1984; Chou et al. 1994) and commercially available analytic software (CalcuSyn for Windows, Biosoft) were used to analyze the experimental data. CI < 1, CI = 1, and CI > 1 quantitatively indicate synergism, additive effect, and antagonism, respectively. The dose-reduction index (DRI) generated by the computer program denotes the folds of dose reduction allowed for each drug in the combination when compared with each agent alone, at a given effect level.

The median-effect equation (Eq.1) is used to calculate the dose effect relationship parameters: $f_a/f_u = (D/D_m)^m$ (Eq.1), which can be rearranged to $D = D_m[f_a/(1 - f_a)]^{1/m}$ where D is dose, D_m is the median-effect dose, f_a and f_u are the fractions inhibited and uninhibited, respectively; D_m is IC_{50} signifying potency, and m denotes the shape of the dose-effect curve in which $m = 1$, >1, and <1 which indicates hyperbolic, sigmoidal, and flat sigmoidal shapes, respectively. The logarithmic form of Eq.1 gives $\log(f_a/f_u) = m\log(D) - m\log(D_m)$ (Eq.2). Therefore, a plot of log (f_a/f_u) *vs* log (D) gives the slope of m value and the antilog of the y-intercept yields the D_m value.

The CI and the DRI can be determined by:

$$CI = \frac{(D)_1}{(D_x)_1} + \frac{(D)_2}{(D_x)_2} \qquad \frac{1}{(DRI)_1} \quad \frac{1}{(DRI)_2} \qquad \text{(Eq. 3)}$$

where D_x is the dose for x% inhibition. For F_a at x% affected by D_1, D_2, or their mixture (i.e., at isoeffective doses) and in the mixture where $(D_x)_{1,2} = (D)_1 + (D)_2$ and $(D)_1/(D)_2 = P/Q$. Substituting Eq. 1 into Eq. 3, produced:

$$CI = \frac{(D_x)_{1,2}[P/(P+Q)]}{(D_m)_1\{(fa_x)_1/1-(fa_x)_1]\}^{1/m_1}} + \frac{(D_x)_{1,2}[Q/(Q-P)]}{(D_m)_2\{(fa_x)_2/1-(fa_x)_2]\}^{1/m_2}} \qquad \text{(Eq. 4)}$$

where $(D_x)_{1,2} = [(fa_x)_{1,2}/[1 - (fa_x)_{1,2}]\}^{1/m_{1,2}}\ [(D_m)_{1,2}]$

and $(fa_x)_1 = (fa_x)_2 = (fa_x)_{1,2}$ (i.e., isoeffective)

Acknowledgments

We thank Conal O'Carroll for his thoughtful suggestions and review of the manuscript, Dr. Susan Naylor for providing the BAC clones used in this study, Dr. Raju S.K. Chaganti for his guidance and assistance with molecular cytogenetic analyses, and Swarna Gogineni for her excellent technical assistance.

The publication costs of this article were defrayed in part by payment of page charges. This article must therefore be hereby marked "advertisement" in accordance with 18 USC section 1734 solely to indicate this fact.

References

Alper, O., De Santis, M.L., Stromberg, K., Hacker, N.F., Cho-Chung, Y.S., and Salomon, D.S. 2000. Anti-sense suppression of epidermal growth factor receptor expression alters cellular proliferation, cell-adhesion, and tumorigenicity in ovarian cancer cells. *Int. J. Cancer* **88:** 566–574.

Bhuyan, D.K., Reddy, P.G., and Bhuyan, K.C. 2000. Growth factor receptor gene and protein expressions in the human lens. *Mech. Aging Dev.* **113:** 205–218.

Bjorkqvist, A.M., Husgafvel-Pursiainen, K., Anttila, S., Karjalainen, A., Tammilehto, L., Mattson, K., Vainio, H., and Knuutila, S. 1998. DNA gains in 3q occur frequently in squamous cell carcinoma of the lung, but not in adenocarcinoma. *Genes Chromosomes Cancer* **22:** 79–82.

Cantley, L.C. and Neel, B.G. 1999. New insights into tumor suppression: PTEN suppresses tumor formation by restraining the phosphoinositide 3-kinase/AKT pathway. *Proc. Natl. Acad. Sci.* **96:** 4240–4245.

Chou, T.C. and Talalay, P. 1984. Quantitative analysis of dose-effect relationships: The combined effects of multiple drugs or enzyme inhibitors. *Adv. Enzyme Regul.* **22:** 27–55.

Chou, T.C., Stepkowski, S.M., and Kahan, B.D. 1994. Computerized quantitation of immunosuppressive synergy for clinical protocol design. *Transplant Proc.* **26:** 3043–3045.

Datta, S.R., Brunet, A., and Greenberg, M.E. 1999. Cellular survival: A play in three Akts. *Genes & Dev. 13:* 2905–2927.

Franke, T.F., Kaplan, D.R., and Cantley, L.C. 1997. PI3K: Downstream AKT action blocks apoptosis. *Cell* **88:** 435–437.

Greenlee, R.T., Murray, T., Bolden, S., and Wingo, P.A. 2000. Cancer statistics, 2000. *CA Cancer J. Clin.* **50:** 7–33.

Henry, M.K., Lynch, J.T., Eapen, A.K., and Quelle, F.W. 2001. DNA damage-induced cell-cycle arrest of hematopoietic cells is overridden by activation of the PI-3 kinase/Akt signaling pathway. *Blood* **98:** 834–841.

Hollstein, M., Soussi, T., Thomas, G., von Brevern, M.C., and Bartsch, H. 1997. p53 gene alterations in human tumors: Perspectives for cancer control. *Recent Results Cancer Res.* **143:** 369–389.

Knuutila, S., Bjorkqvist, A.M., Autio, K., Tarkkanen, M., Wolf, M., Monni, O., Szymanska, J., Larramendy, M.L., Tapper, J., Pere, H., et al. 1998. DNA copy number amplifications in human neoplasms: Review of comparative genomic hybridization studies. *Am. J. Pathol.* **152:** 1107–1123.

Levine, A.J., Chang, A., Dittmer, D., Notterman, D.A., Silver, A., Thorn, K., Welsh, D., and Wu, M. 1994. The p53 tumor suppressor gene. *J. Lab. Clin. Med.* **123:** 817–823.

Liaw, D., Marsh, D.J., Li, J., Dahia, P.L., Wang, S.I., Zheng, Z., Bose, S., Call, K.M., Tsou, H.C., Peacocke, M., et al. 1997. Germline mutations of the PTEN gene in Cowden disease, an inherited breast and thyroid cancer syndrome. *Nat. Genet.* **16:** 64–67.

Ma, Y.Y., Wei, S.J., Lin, Y.C., Lung, J.C., Chang, T.C., Whang-Peng, J., Liu, J.M., Yang, D.M., Yang, W.K., and Shen, C.Y. 2000. PIK3CA as an oncogene in cervical cancer. *Oncogene* **19:** 2739–2744.

Ramaswamy, S., Nakamura, N., Vazquez, F., Batt, D.B., Perera, S., Roberts, T.M., and Sellers, W.R. 1999. Regulation of G_1 progression by the PTEN tumor suppressor protein is linked to inhibition of the phosphatidylinositol 3-kinase/Akt pathway. *Proc. Natl. Acad. Sci.* **96:** 2110–2115.

Sabbatini, P. and McCormick, F. 1999. Phosphoinositide 3-OH kinase (PI3K) and PKB/Akt delay the onset of p53-mediated, transcriptionally dependent apoptosis. *J. Biol. Chem.* **274:** 24263–24269.

Salvesen, H.B., MacDonald, N., Ryan, A., Jacobs, I.J., Lynch,

E.D., Akslen, L.A., and Das, S. 2001. PTEN methylation is associated with advanced stage and microsatellite instability in endometrial carcinoma. *Int. J. Cancer* **91:** 22–26.

Shaw, P., Bovey, R., Tardy, S., Sahli, R., Sordat, B., and Costa, J. 1992. Induction of apoptosis by wild-type p53 in a human colon tumor-derived cell line. *Proc. Natl. Acad. Sci.* **89:** 4495–4499.

Shayesteh, L., Lu, Y., Kuo, W.L., Baldocchi, R., Godfrey, T., Collins, C., Pinkel, D., Powell, B., Mills, G.B., and Gray J.W. 1999. PIK3CA is implicated as an oncogene in ovarian cancer. *Nat. Genet.* **21:** 99–102.

Shinomiya, T., Mori, T., Ariyama, Y., Sakabe, T., Fukuda, Y., Murakami, Y., Nakamura, Y., and Inazawa, J. 1999. Comparative genomic hybridization of squamous cell carcinoma of the esophagus: The possible involvement of the DPI gene in the 13q34 amplicon. *Genes Chromosomes Cancer* **24:** 337–344.

Singh, B., Gogineni, S.K., Sacks, P.G., Shaha, A.R., Shah, J.P., Stoffel, A., and Rao, P.H. 2001. Molecular-cytogenetic characterization of head and neck squamous cell carcinoma and refinement of 3q amplification. *Cancer Res.* **61:** 4506–4513.

Stambolic, V., MacPherson, D., Sas, D., Lin, Y., Snow, B., Jang, Y., Benchimol, S., and Mak, T.W. 2001. Regulation of PTEN transcription by p53. *Mol. Cell* **8:** 317–325.

Stoffel, A., Rao, P.H., Louie, D.C., Krauter, K., Liebowitz, D.N., Koeppen, H., Le Beau, M.M., and Chaganti, R.S. 1999. Chromosome 18 breakpoint in t(11;18)(q21;q21) translocation associated with MALT lymphoma is proximal to BCL2 and distal to DCC. *Genes Chromosomes Cancer* **24:** 156–159.

Wymann, M.P. and Pirola, L. 1998. Structure and function of phosphoinositide 3-kinases. *Biochim. Biophys. Acta.* **1436:** 127–150.

Zhao, N., Stoffel, A., Wang, P.W., Eisenbart, J.D., Espinosa, III, R., Larson, R.A., and Le Beau, M.M. 1997. Molecular delineation of the smallest commonly deleted region of chromosome 5 in malignant myeloid diseases to 1–1.5 Mb and preparation of a PAC-based physical map. *Proc. Natl. Acad. Sci.* **94:** 6948–6953.

Zhao, R., Gish, K., Murphy, M., Yin, Y., Notterman, D., Hoffman, W.H., Tom, E., Mack, D.H., and Levine, A.J. 2000. Analysis of p53-regulated gene expression patterns using oligonucleotide arrays. *Genes & Dev.* **14:** 981–993.